Self-assembling resorcinarene capsules: solid and gas phase studies on encapsulation of small alkyl ammonium cations

Heidi Mansikkamäki,[a] Maija Nissinen,[a] Christoph A. Schalley[b] and Kari Rissanen*[a]

[a] *Department of Chemistry, University of Jyväskylä, PO Box 35, FIN-40014,*
University of Jyväskylä, Finland. E-mail: hemansik@st.jyu.fi, majoni@cc.jyu.fi,
kari.rissanen@jyu.fi; Fax: +358 14 260 2501; Tel: +358 14 260 2672
[b] *Kekulé-Institut für Organische Chemie und Biochemie der Universität, Gerhard-Domagk-Str. 1,*
D-53121 Bonn, Germany. E-mail: c.schalley@uni-bonn.de

Received (in Montpellier, France) 9th August 2002, Accepted 25th September 2002
First published as an Advance Article on the web 8th November 2002

The self-assembling process of unsubstituted resorcinarenes (**1**, **2** and **3**) to dimeric capsules encapsulating small tetra-alkyl ammonium cations **4**–**7** has been studied in solid and gaseous states by X-ray crystallographic and mass spectrometric methods. Hydrogen bonding and cation-π interaction as well as the proper encapsulation in the empty cavity of the capsule appear to be the most important interactions in the capsule formation process. Competitive mass spectrometric studies clearly indicated preference of the tetramethyl ammonium cation (**4**) over tetraethyl ammonium cation (**6**) and especially tetrabutyl ammonium cation (**7**). The crystal structures of altogether eight dimeric capsules of resorcinarenes **1**–**3** with cations **4** and **5** were determined. In the solid state, the alkyl chain length of the host affects the crystal packing significantly. However, ethyl resorcinarene (**2**) is the only host, which binds the spherical halide anion (Cl^- or Br^-) in between the lower rim alkyl chains.

Introduction

Recently, supramolecular reversible encapsulation and self-assembling molecular aggregates with molecular recognition properties have attracted worldwide interest.[1] These objectives are met with resorcinarenes which are versatile and easily available host compounds for complexation studies in solution, in the gas phase and in the solid state.[2] One of the most interesting and elegant features of unsubstituted alkyl resorcinarenes is their capability to form dimeric[3] and hexameric[4] molecular capsules/containers encapsulating neutral and/or charged guests inside the cavity.

The studies of the complexation of alkyl ammonium cations, *e.g.* biologically significant acetylcholine,[5a] by resorcinarenes and their tetraphenolate derivatives have demonstrated the complexation of suitably sized ammonium cations.[3,5,6] Our recent interest is focused on the self-assembling hydrogen-bonded capsule formation process and recognition properties of unsubstituted alkyl resorcinarenes by complexation and encapsulation of ammonium cations. The complexation owes mainly to the electrostatic attraction between the π-basic cavity of the resorcinarene capsule and the size of the positively charged cation.

Most of the early studies manifest monomeric 1:1 complexation, while 2:1 complexation to dimeric capsules encapsulating alkyl ammonium cations has been observed in solid state studies.[3] These studies emphasize the significance of the cation size for successful encapsulation, while the effect of the counterion and solvent is small.[3,6] Recently, we have observed an interesting simultaneous encapsulation of diquats concomitant with binding of spherical anions such as Cl^- and Br^- as a bridge between the lower rim ethyl chains of ethyl resorcinarene (**2**).[3d]

In the previous studies,[3a–c] the dimeric capsule was reported to be eclipsed, yet our most recent study[3d] revealed the formation of a staggered capsule. Gas phase studies[6] have indicated the possibility of obtaining directly hydrogen-bonded capsules without solvent or anion mediation, an interesting feature, which we believe to be achievable also in solid state when suitable crystallisation conditions are found.

The mass spectrometric examination of non-covalently bound supramolecular aggregates[7] is not always straightforward. In particular, hydrogen-bonded aggregates often cause problems due to the use of competitive or even protic solvents or matrices. Nevertheless, several successful examples for such systems have been reported, among them rosette-type complexes,[8] molecular boxes,[9] hydrogen-bonded ferrocene oligomers,[10] and self-assembling capsules.[11] As a bottom line of all these studies, it is still a challenge to the imagination of the researcher to find suitable conditions for ionisation. If non-competitive conditions have to be used, it is advantageous to pre-generate the ions of interest in solution or the matrix before ionisation. This can be done by covalent addition of a crown ether–alkali metal ion complex[8a] or by attachment of an anion to the hydrogen bonding system[8b,c] as long as it does not destroy or alter the binding between the subunits too much. Other possibilities include sandwich complexes of Ag^+ ions[9] or the oxidation of ferrocene units by addition of iodine to the sample just before the ESI-MS experiment.[10] In the case of capsules, which accept guests inside their cavity, this guest, *e.g.* a quaternary ammonium ion can of course be charged.[11] Calixarene- and resorcinarene-based hydrogen-bonded capsules and the corresponding monomeric complexes have been the subject of several previous studies,[6,12] some of which belong to the earliest examples for true gas-phase complexation studies.[13]

Based on the previously obtained results in solid and gaseous states, we wanted to study the factors influencing the ammonium cation induced self-assembly to dimeric capsules by investigating systematically the significance of the cation and anion size. The alkyl chain length was varied to survey the anion binding properties of the lower rim and packing of

DOI: 10.1039/b207875a

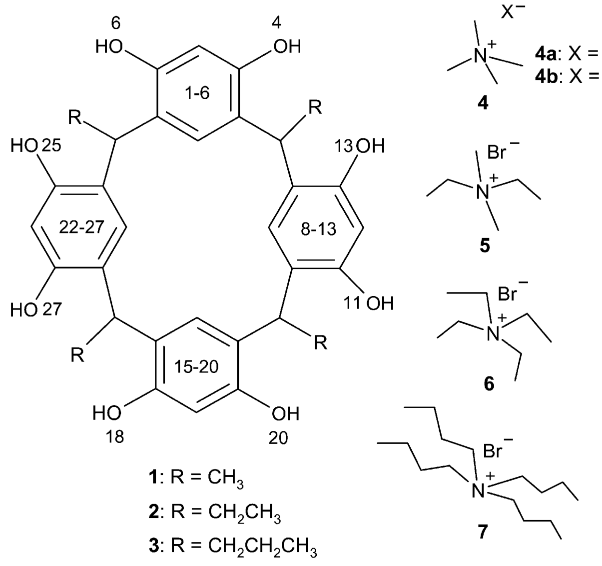

Scheme 1 Structural formulae and relevant crystallographic numbering of resorcinarenes.

the capsules in the crystal lattice. The solid state studies were performed to find out the detailed structures of the capsules. In the mass spectral studies, the data obtained for the capsules with singly charged guest ions will be discussed; particular focus will be on the determination of structural features of these compounds.

Results and discussion

X-Ray crystallography and solid state capsules

Crystallisation studies. The solid state complexation and encapsulation properties of the alkyl resorcinarenes **1**, **2** and **3** with alkyl ammonium salts **4** and **5** were studied systematically in crystallisation studies from aqueous methanol and ethanol solutions using a 2:1 host to guest molar ratio (Scheme 1, Table 1). Altogether 18 crystallisation experiments were performed. Of these 15 produced capsules, eight of which are reported in this paper. The seven remaining capsules are not reported here, due to the bad quality of crystals and hence the quality of the data obtained. Here, the results of these seven are only considered as preliminary[15] (recrystallisations to get better data are currently in progress).

Capsule of methyl resorcinarene 1. Co-crystallisation of **1** with **4b** in aqueous methanol resulted in pale hexagonal crystals of composition $\mathbf{4}^+@\mathbf{1}_2\cdot\mathrm{Br}^-\cdot 4\mathrm{MeOH}\cdot 3\mathrm{H_2O}$. Other attempts to crystallise **1** either with **4a** or **5** in MeOH resulted in a microcrystalline powder precipitate.

In the capsule, $\mathbf{4}^+@\mathbf{1}_2\cdot\mathrm{Br}^-\cdot 4\mathrm{MeOH}\cdot 3\mathrm{H_2O}$, two molecules of **1** are linked *via* MeOH molecules, water molecules and bromide (disordered over two positions with one of the water molecules) and, as expected, the TMA cation ($\mathbf{4}^+$) is located inside the cavity formed by the resorcinarene hosts (Fig. 1). The distances of the methyl groups of the cation to the centroids of the aromatic groups of the resorcinarene host (3.41 and 3.62 Å) indicate C–H···π interaction between the host and the guest. The resorcinarene molecules adopt a slightly distorted cone conformation that is flattened on the sides where the Br^- anion is mediating the capsule (Table 2). The capsule is staggered and slightly tighter, *i.e.* the capsule halves are slightly closer to each other than in our previous study with diquats,[3d] due to the smaller size of the cation, the distance between the planes defined by the methine bridges of the hosts being 8.36 Å. Survey of the crystal packing reveals perpendicular columns formed by sequential capsules (Fig. 2).

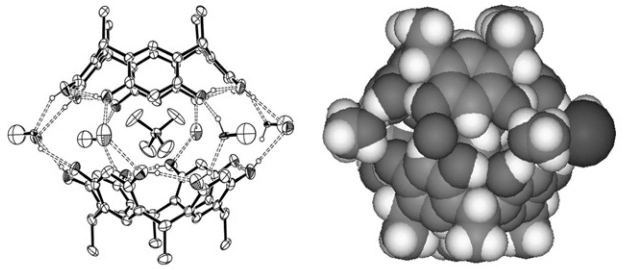

Fig. 1 Ortep[16] and CPK plots of the X-ray structure of hydrogen-bonded solvent–anion mediated resorcinarene **1** capsule $\mathbf{4}^+@\mathbf{1}_2\cdot\mathrm{Br}^-\cdot 4\mathrm{MeOH}\cdot 3\mathrm{H_2O}$. Non-hydrogen bonding molecules have been omitted for clarity from the Ortep plot.

Preliminary crystallisation studies indicate encapsulation of both cations $\mathbf{4}^+$ and $\mathbf{5}^+$ in dimeric **1** in aqueous ethanol solution,[15] but owing to the poor quality and instability of crystals formed, good enough X-ray data could not be obtained from either of them.

Capsules of ethyl resorcinarene 2. Dimeric capsules of **2** of composition $\mathbf{4}^+@\mathbf{2}_2\cdot\mathrm{Cl}^-\cdot 6\mathrm{MeOH}\cdot\mathrm{H_2O}$, $\mathbf{4}^+@\mathbf{2}_2\cdot\mathrm{Cl}^-\cdot 4.5\mathrm{H_2O}$ and $\mathbf{4}^+@\mathbf{2}_2\cdot\mathrm{Br}^-\cdot 8\mathrm{MeOH}$ (Fig. 3) were successfully obtained by crystallisation with TMA chloride **4a** in both methanol and ethanol and with TMA bromide **4b** in methanol. The preliminary results of the crystallisation of **4b** from ethanol and dimethyl diethyl ammonium bromide (**5**) (Table 1) also indicated capsule formation, but again owing to the inferior quality of the data obtained, no definite conclusions about the structures could be made.[15]

The two capsules $\mathbf{4}^+@\mathbf{2}_2\cdot\mathrm{Cl}^-\cdot 6\mathrm{MeOH}\cdot\mathrm{H_2O}$ and $\mathbf{4}^+@\mathbf{2}_2\cdot\mathrm{Br}^-\cdot 8\mathrm{MeOH}$ obtained from methanol resemble closely the earlier results of the pair of capsules of **2** with larger diquats 1,4-diazoniabicyclo[2.2.2]octane dichloride and 1,4-dimethyl-1,4-diazoniabicyclo[2.2.2]octane dibromide,[3d] the first one being staggered and anion–solvent mediated and the latter one being eclipsed and only methanol mediated. However, in this case the cation is the same in both structures, thus the structure of the capsule cannot be explained by the size of the cation, but most probably the staggered structure relates to the

Table 1 Crystallisation experiments of resorcinarenes **1**, **2** and **3** with alkyl ammoniumsalts **4a**, **4b** and **5** in aqueous methanol and ethanol

	Solvent	**1**	**2**	**3**
4a	MeOH	Powder precipitate	$\mathbf{4}^+@\mathbf{2}_2\cdot\mathrm{Cl}^-\cdot 6\mathrm{MeOH}\cdot\mathrm{H_2O}$	$\mathbf{4}^+@\mathbf{3}_2\cdot\mathrm{Cl}^-\cdot 4\mathrm{MeOH}$
	EtOH	Capsule[a]	$\mathbf{4}^+@\mathbf{2}_2\cdot\mathrm{Cl}^-\cdot 4.5\mathrm{H_2O}$	$\mathbf{4}^+@\mathbf{3}_2\cdot\mathrm{Cl}^-\cdot 4\mathrm{EtOH}$
4b	MeOH	$\mathbf{4}^+@\mathbf{1}_2\cdot\mathrm{Br}^-\cdot 4\mathrm{MeOH}\cdot 3\mathrm{H_2O}$	$\mathbf{4}^+@\mathbf{2}_2\cdot\mathrm{Br}^-\cdot 8\mathrm{MeOH}$	Powder precipitate
	EtOH	Capsule[a]	Capsule[a]	$\mathbf{4}^+@\mathbf{3}_2\cdot\mathrm{Br}^-\cdot 4\mathrm{EtOH}$
5	MeOH	Powder precipitate	Capsule[a]	$\mathbf{5}^+@\mathbf{3}_2\cdot\mathrm{Br}\cdot\mathrm{MeOH}\cdot 0.5\mathrm{H_2O}$
	EtOH	Capsule[a]	Capsule[a]	Capsule[a]

[a] Preliminary results.

Table 2 Capsule dimensions in solid state structures

Capsule	$\mathbf{4}^+@\mathbf{1}_2\text{Br}^-\cdot 4\text{MeOH}\cdot 3\text{H}_2\text{O}$	$\mathbf{4}^+@\mathbf{2}_2\cdot\text{Cl}^-\cdot 6\text{MeOH}\cdot\text{H}_2\text{O}$	$\mathbf{4}^+@\mathbf{2}_2\cdot\text{Cl}^-\cdot 4.5\text{H}_2\text{O}$	$\mathbf{4}^+@\mathbf{2}_2\cdot\text{Br}^-\cdot 8\text{MeOH}$	$\mathbf{4}^+@\mathbf{3}_2\cdot\text{Cl}^-\cdot 4\text{MeOH}$	$\mathbf{4}^+@\mathbf{3}_2\cdot\text{Cl}^-\cdot 4\text{EtOH}$	$\mathbf{4}^+@\mathbf{3}_2\cdot\text{Br}^-\cdot 4\text{EtOH}$	$\mathbf{5}^+@\mathbf{3}_2\cdot\text{Br}^-\cdot 4\text{MeOH}\cdot 0.5\text{H}_2\text{O}$
Capsule mediating hydrogen bonds to solvents/Å	2.62–3.12	2.64–2.86	2.69–2.91	2.67–2.69	2.68–2.88	2.66–2.74	2.66–2.75	2.60–2.72
Capsule mediating hydrogen bonds to anions/Å	3.10	2.86	3.04	—	3.07–3.79	3.11–3.14	3.23, 3.25	3.23
Distance between the capsule halves/Å[a]	8.36	8.77, 8.80[c]	8.35	8.86	8.34	8.53	8.59	8.98
Distance between the centroids of opposite aromatic rings of a resorcinarene molecule/Å	6.62/7.11	6.62/7.07 6.61/7.07[c]	6.71/6.99	6.87/6.87	6.88/6.90	6.77/6.99	6.79/6.97	6.86/6.95
C–H···π interactions between cation and resorcinarenes/Å	3.40–4.47	3.50–3.77	3.33–4.22	3.36–3.86	3.45–4.03	3.16–4.04	3.35–4.04	3.64–3.96
Torsion angle between the capsule halves/°[b]	40.4	42.8	40.0	0.0	34.8	0.1	0.1	0.1
Number of intra/inter molecular hydrogen bonds	4/16	3/16	4/13	4/12	4/12	4/12	4/12	4/13

[a] Defined as a distance between the planes formed by the methine bridges of the resorcinarenes. [b] The angle is measured as a torsion angle between lower rim methine carbon of the upper host, centroid of the plane defined by methine carbons of the upper host, corresponding centroid of the lower host and the closest methine carbon of the lower host. [c] Asymmetric unit contains two unequal halves of the capsule.

capsule-mediating role of the anion. The role of the anions in crystal packing is also similar to the previously observed diquat capsules, *i.e.* the anions of $\mathbf{4}^+@\mathbf{2}_2\cdot\text{Cl}^-\cdot 6\text{MeOH}\cdot\text{H}_2\text{O}$ and $\mathbf{4}^+@\mathbf{2}_2\cdot\text{Br}^-\cdot 8\text{MeOH}$ are found in between the lower rim ethyl chains of the resorcinarene host and in the former capsule the anion is simultaneously mediating the capsule halves (Fig. 3 and ref. 3d).

When **2** was crystallised with **4a** from aqueous ethanol, capsule $\mathbf{4}^+@\mathbf{2}_2\cdot\text{Cl}^-\cdot 4.5\text{H}_2\text{O}$ mediated by 4.5 water molecules and two chloride anions resulted, which means that on average 13 intracapsular hydrogen bonds are formed. No ethanol is present in the crystal, although only a trace of water was used in the crystallisation. The orientation of the capsule is eclipsed, which most probably relates to the small size of the mediating solvents and the capsule-mediating role of chloride.

In both staggered capsules $\mathbf{4}^+@\mathbf{2}_2\cdot\text{Cl}^-\cdot 6\text{MeOH}\cdot\text{H}_2\text{O}$ and $\mathbf{4}^+@\mathbf{2}_2\cdot\text{Cl}^-\cdot 4.5\text{H}_2\text{O}$, the conformation of the resorcinarenes is slightly distorted, while the conformation of resorcinarenes in eclipsed capsule $\mathbf{4}^+@\mathbf{2}_2\cdot\text{Br}^-\cdot 8\text{MeOH}$ is near perfect (Table 2). The reason for this is the fact that the capsule mediating solvents consist only of methanol molecules, while the chlorides mediating the dimerisation cause a distortion from the perfect conformation in staggered capsules.

In all three capsules of **2**, the cation is tightly embedded inside the capsule. Complex-stabilising C–H···π interactions between aromatic parts of the host and the guest are evident on the basis of the closest distances between the methyl groups of the cation and the centroids of the aromatic resorcinol groups (3.33–3.86 Å).

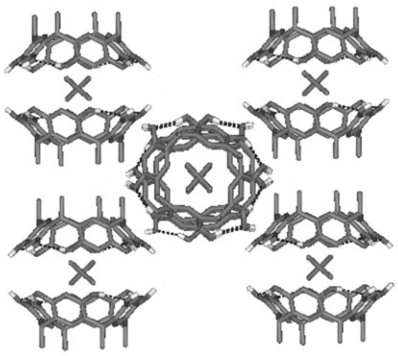

Fig. 2 Crystal packing of $\mathbf{4}^+@\mathbf{1}_2\cdot\text{Br}^-\cdot 4\text{MeOH}\cdot 3\text{H}_2\text{O}$ showing the perpendicular columns formed by sequential resorcinarene capsules. Solvent molecules, anions and non-hydrogen bonding hydrogens are omitted for clarity.

All three capsules have a different type of packing pattern. The packing of capsule $\mathbf{4}^+@\mathbf{2}_2\cdot\text{Br}^-\cdot 8\text{MeOH}$ builds up of parallel columns formed by sequential capsules, the interstice of which is filled by a hydrogen-bonded bromide–methanol network (Fig. 4).

Capsule $\mathbf{4}^+@\mathbf{2}_2\cdot\text{Cl}^-\cdot 6\text{MeOH}\cdot\text{H}_2\text{O}$ reveals a similar crystal packing as the capsule of **2** with 1,4-diazoniabicyclo[2.2.2]octane dichloride reported by us previously.[3d] In both capsules, the chloride anions are mediating the mutual binding of the two capsule halves and are simultaneously located between the lower rim ethyl chains of the adjacent perpendicularly positioned capsules. Capsule $\mathbf{4}^+@\mathbf{2}_2\cdot\text{Cl}^-\cdot 4.5\text{H}_2\text{O}$ has a similar type of crystal packing when compared to the capsules of propyl resorcinarene (**3**) (Fig. 6), and is discussed in the following paragraph.

Capsules of propyl resorcinarene 3. Three solid state capsules of **3** with **4**, ($\mathbf{4}^+@\mathbf{3}_2\cdot\text{Cl}^-\cdot 4\text{MeOH}$, $\mathbf{4}^+@\mathbf{3}_2\cdot\text{Cl}^-\cdot 4\text{EtOH}$ and $\mathbf{4}^+@\mathbf{3}_2\cdot\text{Br}^-\cdot 4\text{EtOH}$) and one of **3** with **5** ($\mathbf{5}^+@\mathbf{3}_2\cdot\text{Br}^-\cdot 4\text{MeOH}\cdot 0.5\text{H}_2\text{O}$) were determined (Table 1). All four capsules of **3** are mediated by two anions (bromide or chloride depending on the salt used) and four solvent molecules (Fig. 5). In $\mathbf{5}^+@\mathbf{3}_2\cdot\text{Br}^-\cdot 4\text{MeOH}\cdot 0.5\text{H}_2\text{O}$, an additional water molecule (population parameter 0.5) participates in capsule formation.

Three capsules out of four ($\mathbf{4}^+@\mathbf{3}_2\cdot\text{Cl}^-\cdot 4\text{EtOH}$, $\mathbf{4}^+@\mathbf{3}_2\cdot\text{Br}^-\cdot 4\text{EtOH}$ and $\mathbf{5}^+@\mathbf{3}_2\cdot\text{Br}^-\cdot 4\text{MeOH}\cdot 0.5\text{H}_2\text{O}$) formed from the host **3** possess an eclipsed orientation and have similar unit cell dimensions, $\mathbf{4}^+@\mathbf{3}_2\cdot\text{Cl}^-\cdot 4\text{EtOH}$ and $\mathbf{4}^+@\mathbf{3}_2\cdot\text{Br}^-\cdot 4\text{EtOH}$ being isomorphous. The only capsule in staggered orientation is $\mathbf{4}^+@\mathbf{3}_2\cdot\text{Cl}^-\cdot 4\text{MeOH}$. The reason for favoured eclipsed orientation is in $\mathbf{4}^+@\mathbf{3}_2\cdot\text{Cl}^-\cdot 4\text{EtOH}$ and $\mathbf{4}^+@\mathbf{3}_2\cdot\text{Br}^-\cdot 4\text{EtOH}$ the larger size of the capsule mediating ethanol molecules compared to methanol or water and in $\mathbf{5}^+@\mathbf{3}_2\cdot\text{Br}^-\cdot 4\text{MeOH}\cdot 0.5\text{H}_2\text{O}$ the larger size of the cation inside the capsule.

Surprisingly, in the capsule $\mathbf{4}^+@\mathbf{3}_2\cdot\text{Cl}^-\cdot 4\text{MeOH}$ with staggered orientation the resorcinarene molecules possess the most symmetrical conformation despite the distorting effect of the mediating anions described above, while the conformation of the resorcinarenes is slightly distorted in eclipsed oriented capsules of **3** (Table 2). As expected the staggered capsule is the

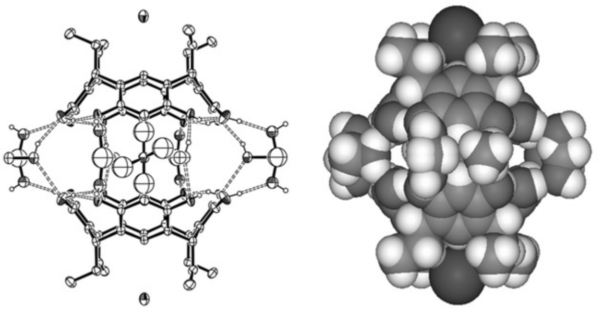

4$^+$@**2**$_2$·Br$^-$·8MeOH

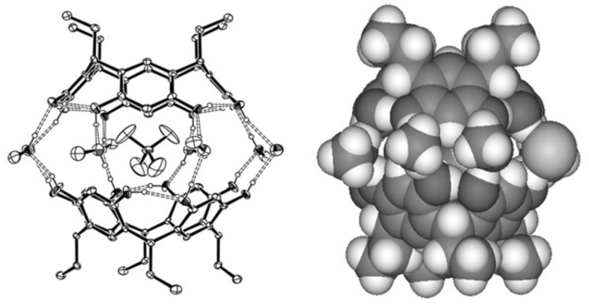

4$^+$@**2**$_2$·Cl$^-$·6MeOH·H$_2$O

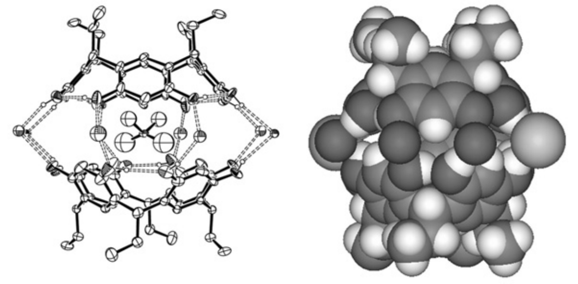

4$^+$@**2**$_2$·Cl$^-$·4.5H$_2$O

Fig. 3 X-ray structures of the resorcinarene capsules of **2**. **4**$^+$@**2**$_2$·Br$^-$·8MeOH is mediated *via* methanol molecules, **4**$^+$@**2**$_2$·Cl$^-$·6MeOH·H$_2$O is methanol–anion mediated and **4**$^+$@**2**$_2$·Cl$^-$·4.5H$_2$O water–anion mediated. In capsule **4**$^+$@**2**$_2$·Cl$^-$·6MeOH·H$_2$O, the anion is simultaneously found in between the ethyl chains (see Fig. 2 in ref. 3d). Non-hydrogen-bonded hydrogen atoms are omitted for clarity from Ortep[15] pictures. Only one of the crystallographically independent capsule halves is shown in the picture of **4**$^+$@**2**$_2$·Cl$^-$·6MeOH·H$_2$O.

tightest one, *i.e.* the distance between the planes defined by the methine bridges is 8.34 Å, and the loosest is **5**$^+$@**3**$_2$·Br$^-$·4MeOH·0.5H$_2$O with the larger size cation (8.98 Å).

The disordered cations are embedded inside the capsules of **3** and cation **5**$^+$, which attracts interest due to its larger size, lies in a horizontal position inside the cavity of the capsule. The horizontal position is similar to the position of 1,4-dimethyl-1,4-diazoniabicyclo[2.2.2]octane[3d] and tetraethyl ammonium cation[3a] observed earlier. C–H···π and cation-π interactions play a noticeable role also in these capsules, since the closest distances between carbon atoms of the cations and the electron rich face of the aromatic rings of the host vary from 3.35 to 4.04 Å.

An exceptional feature of the structures obtained from **2** is the location of the anions at the interstices between adjacent capsules rather than between the lower rim alkyl chains. At these positions, they simultaneously are capable of linking the two capsule halves together (Fig. 6).

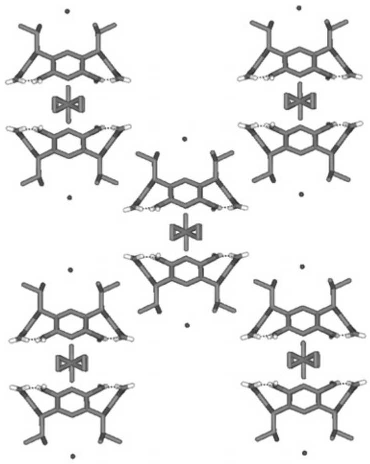

Fig. 4 Crystal packing pattern of **4**$^+$@**2**$_2$·Br$^-$·8MeOH. Non-hydrogen bonding hydrogens and disordered solvent molecules filling the interstice are excluded for clarity.

All four capsules of **3** and one capsule of **2** (**4**$^+$@**2**$_2$·Cl$^-$·4.5H$_2$O) have similar crystal packing patterns. The packing of **4**$^+$@**3**$_2$·Br$^-$·4EtOH is shown in Fig. 6 and discussed here in more detail to represent all of the structures mentioned above. The adjacent molecular capsules in **4**$^+$@**3**$_2$·Br$^-$·4EtOH ·4EtOH are connected *via* capsule mediating anions to form side to side hydrogen-bonded continuous chains. The capsule ribbons next to each other are placed so that the aliphatic alkyl chains of resorcinarenes are pointing towards the alkyl chains of the adjacent resorcinarene. This leads to the formation of hydrophobic and hydrophilic layers in the crystal.

Comparison of the structures of the capsules of 1, 2 and 3. Encapsulation of small alkyl ammonium cations is favourable for all three resorcinarenes (**1**, **2** and **3**) used in crystallisation experiments. The lack of anion binding ability in between the alkyl chains of **1** and **3** indicates that only **2** has a suitably sized binding place for spherical anions at the lower rim, while the alkyl chains of **1** are too short and the longer chains of **3** already start to form hydrophobic layers in the crystals. It needs to be pointed out that methyl resorcinarene, **1**, gave a powder precipitate when crystallised with **4a** and **5** in methanol and no reliable extensive conclusions can be made on the basis of the only capsule of **1**. The capsules of **3** are all similarly anion–solvent mediated and have the same packing pattern while capsules of **2** have the greatest variety of different capsule structures and types of crystal packing.

Mass spectrometric investigation of singly charged capsules

ESI mass spectrometry. Acetonitrile solutions of compounds **1**–**3** containing quaternary ammonium salts give clean ESI mass spectra, as shown in Fig. 7 for tetra methyl ammonium bromide. Besides intense signals for the monomer–guest complexes **4**$^+$@**1**–**4**$^+$@**3** (m/z 618, 674, and 730, respectively; traces a–c), dimeric complexes **4**$^+$@**1**$_2$–**4**$^+$@**3**$_2$ are observed at m/z 1162, 1274, and 1387. These ions combine two resorcinarenes and one ammonium ion in one singly charged complex. The isotope patterns determined in the experiment reveal a peak spacing of $\Delta m = 1$ amu and are in perfect agreement with those calculated for these complexes based on natural isotope abundances (see inset). This confirms the elemental composition of the complex as well as its singly charged nature. Some other ions appearing in the spectra as low-intensity signals are mostly due to salt clustering. To our experience, acetonitrile is the best solvent choice. Test experiments with acetone or even more unpolar solvents caused solubility problems with the

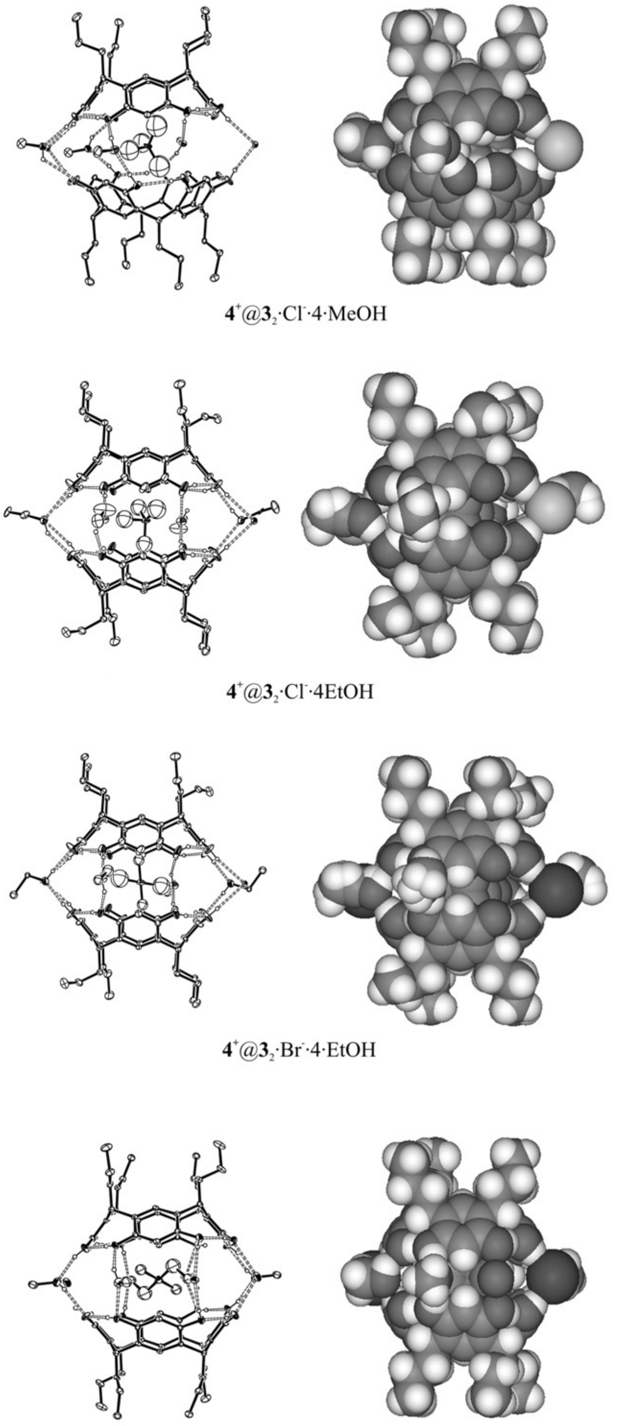

$\mathbf{4}^{+}@\mathbf{3}_{2}\cdot\mathrm{Cl}^{-}\cdot4\cdot\mathrm{MeOH}$

$\mathbf{4}^{+}@\mathbf{3}_{2}\cdot\mathrm{Cl}^{-}4\mathrm{EtOH}$

$\mathbf{4}^{+}@\mathbf{3}_{2}\cdot\mathrm{Br}^{-}\cdot4\cdot\mathrm{EtOH}$

$\mathbf{5}^{+}@\mathbf{3}_{2}\cdot\mathrm{Br}^{-}4\mathrm{MeOH}\cdot0.5\mathrm{H_2O}$

Fig. 5 X-ray structures of resorcinarene **3** capsules have great similarity to each other. All capsules are solvent–anion mediated. Non-hydrogen-bonded atoms have been omitted for clarity from Ortep plots.

guest salts which could probably be overcome if more weakly bonding anions were used such as $\mathrm{BF_4}^-$ or $\mathrm{PF_6}^-$. Protic solvents like methanol, however, generate significant amounts of protonated ions unnecessarily obscuring the spectra with additional signals.

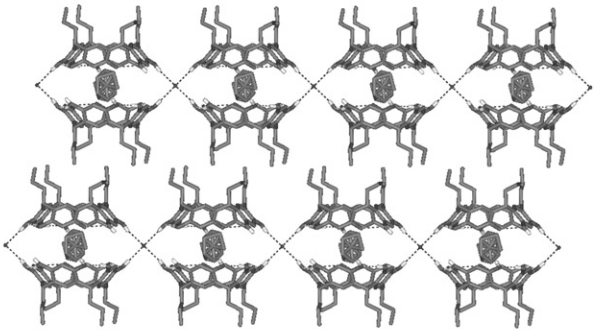

a) frontview

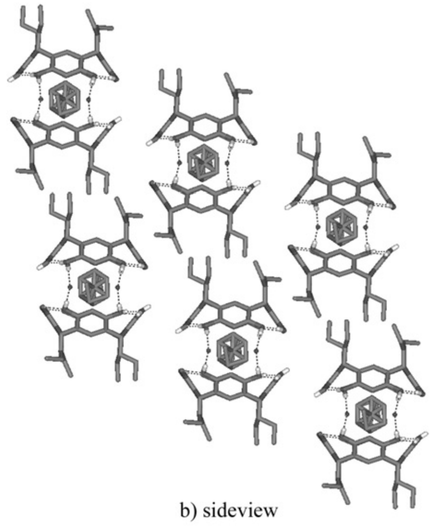

b) sideview

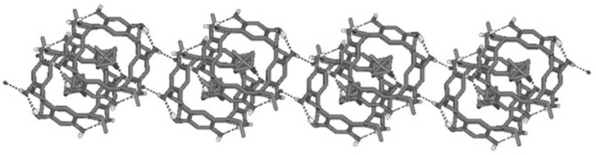

c) topview

Fig. 6 Crystal packing of structure $\mathbf{4}^{+}@\mathbf{3}_{2}\cdot\mathrm{Br}^{-}\cdot4\mathrm{EtOH}$. Adjacent capsules are hydrogen-bonded to each other *via* capsule mediating anions (a and c). Hydrophilic and hydrophobic layers are formed due to the propyl chains of the resorcinarene that start to govern the crystal packing (b). Non-hydrogen bonding hydrogens and solvent molecules are omitted for clarity.

Mass spectral evidence for heterodimer formation. Equimolar mixtures of two different resorcinarenes (Fig. 7d–f) with $\mathbf{4}^{+}\mathrm{Br}^{-}$ as the guest salt gave not only signals for the homodimers, but also new signals for the heterodimers $\mathbf{4}^{+}@\mathbf{1}\cdot\mathbf{2}$ (m/z 1218), $\mathbf{4}^{+}@\mathbf{1}\cdot\mathbf{3}$ (m/z 1275), and $\mathbf{4}^{+}@\mathbf{2}\cdot\mathbf{3}$ (m/z 1331). The heterodimers are almost twice as abundant as the homodimers – as expected from statistics. Some minor deviation from the exact statistical ratio may either be due to the instrument parameters or to different ionisation efficiencies depending on the length of the solubilising side chains at the bottom rims of the resorcinarenes, but of course do not alter the qualitative picture. The existence of heterodimers indicates that the complexes are reversibly formed by non-covalent interactions. Since the relative intensities did not change over time, even, when two stock solutions each with only one of the resorcinarenes were directly mixed before the experiment, the exchange of monomers is fast and complete equilibrium is reached within less than one minute.

Competition studies to assess capsule size selectivity. It is often rather difficult to obtain structural information on such supramolecular complexes from mass spectrometric experiments. The crystallographic part of this work strongly points to the formation of capsules. However, there is a huge

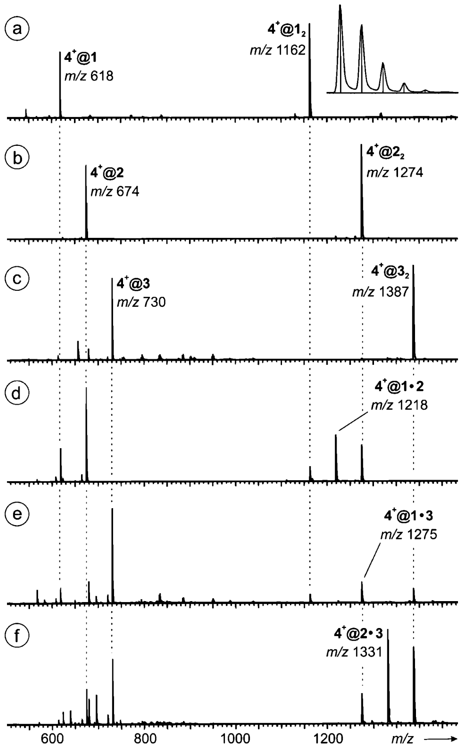

Fig. 7 ESI mass spectra of 50 μM acetonitrile solutions of (a) **1**, (b) **2**, and (c) **3** with equimolar amounts of salt tetramethyl ammonium bromide **4**$^+$Br$^-$ providing the guest ion. Spectra (d)–(f) were obtained from mixtures of (d) **1** and **2**, (e) **1** and **3**, and (f) **2** and **3**, 25 μM in each host monomer and 50 μM in **4**$^+$Br$^-$. The inset in spectrum (a) shows the recorded isotope pattern (curve) for **4**$^+$@**2**$_2$ in comparison to that calculated on the basis of natural isotope abundances (vertical lines).

difference between the capsules in the solid state and the gas phase: While solvent molecules or anions serve for bridging the two halves, in the gas phase such bridges do not exist. Of course, other structures than that of a cation-filled capsule are not beyond imagination. For example, an empty capsule with an ammonium ion attached to the outer surface does not seem unreasonable. Open structures would of course suffer from a loss of binding energy due to cleavage of at least part of the hydrogen bonds between the two halves. In contrast to the crystals, where solvent molecules enlarge the cavity volumes of the capsules by extending the hydrogen bonding pattern, these solvent molecules – if present in solution at all – are likely stripped off during the electrospray process. One would thus expect the dimer to form a somewhat smaller, "collapsed" capsule in the gas phase without these bridges. Consequently, one might also expect a distinct preference for smaller ammonium ions if the ions are inside a hydrogen-bonded capsule with an intact seam of hydrogen bonds. Similar arguments have earlier been successfully used to infer the structure for hydrogen-bonded self-assembling capsules indirectly by mass spectrometric means.[11,14] Competition experiments with guests of different sizes have been performed. One of the problems associated with these experiments is that the guests should be present in large excess in order to realize a true competition. However, high salt concentrations lead to decreased signal intensities for the desired complex ions. Instead, intense signals for salt clusters are observed. As a compromise, the solutions used to obtain the spectra in Fig. 8 contained four equivalents of each guest salt relative to the dimeric capsule. This should at least allow us to obtain qualitative information.

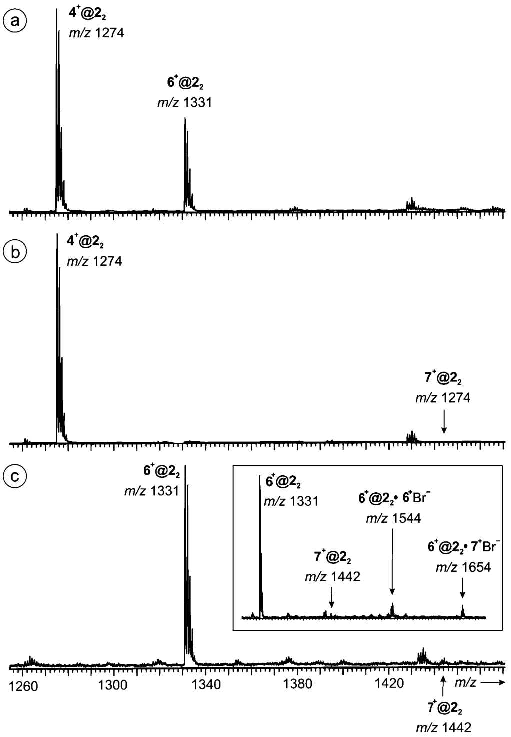

Fig. 8 Competition of guests (a) **4**$^+$Br$^-$ and **5**$^+$Br$^-$, (b) **4**$^+$Br$^-$ and **6**$^+$Br$^-$, and (c) **6**$^+$Br$^-$ and **7**$^+$Br$^-$ for host **2**$_2$. Note that only the region is shown in which the dimer–guest complexes are observed. All sample solutions were 50 μM with respect to the host monomer and 100 μM with respect to each guest salt. Higher excesses of the salts result in reduced signal intensities for the desired dimer–guest complexes. Instead, salt clusters become more prominent. The inset in the bottom spectrum shows two salt adducts to **6**$^+$@**2**$_2$. Ion pairs of both salts present in the mixture are attached to this ion with similar abundance (**6**$^+$@**2**$_2$·**6**$^+$Br$^-$ *versus* **6**$^+$@**2**$_2$·**7**$^+$Br$^-$), while there is a strong preference for **6**$^+$@**2**$_2$ over **7**$^+$@**2**$_2$.

Indeed, the spectrum of an equimolar mixture of tetramethyl and tetraethyl ammonium bromides **4**$^+$Br$^-$ and **6**$^+$Br$^-$ with resorcinarene **2** gave intense signals for both dimer–guest complexes with a 2:1 preference for **4**$^+$@**2**$_2$ over **6**$^+$@**2**$_2$. Thus, the expected preference for ammonium ions smaller than those utilized in the crystallographic work is indeed observed. Similar experiments with either one of these two salts competing for complexation with tetrabutyl ammonium bromide **7**$^+$Br$^-$ only gave rise to signals for dimer–guest complexes containing the smaller cation. Signals for **7**$^+$@**2**$_2$ almost completely vanish within the noise.

Even more surprising is the formation of two salt adducts with low, but almost equal intensity (inset in Fig. 9): **6**$^+$@**2**$_2$·**6**$^+$Br$^-$ (*m*/*z* 1544) and **6**$^+$@**2**$_2$·**7**$^+$Br$^-$ (*m*/*z* 1654). The third expected salt-adduct **7**$^+$@**2**$_2$·**7**$^+$Br$^-$ bearing two large tetrabutyl ammonium cations is again not observed. These findings strongly point to the existence of hydrogen-bonded capsular ions carrying the **6**$^+$ guest ion inside their cavity, while the additional ion pair is attached to the outer surface. While there is a strong preference for the smaller cation in the dimer–guest complexes, no such preference is seen when an additional ion pair is attached outside. The size selectivity, although only qualitatively examined here, strongly points to the formation of capsules that remain intact on their way into the gas phase.

The gas-phase structure: still a capsule?. The arguments put forward so far are not quite conclusive with respect to the structure in the gas phase. One might argue that such ESI-MS experiments might only monitor the situation in solution, while in the gas phase the structure might be destroyed. Indeed, any kind of rearrangement that would just arrange the subunits differently without fragmentation would give rise

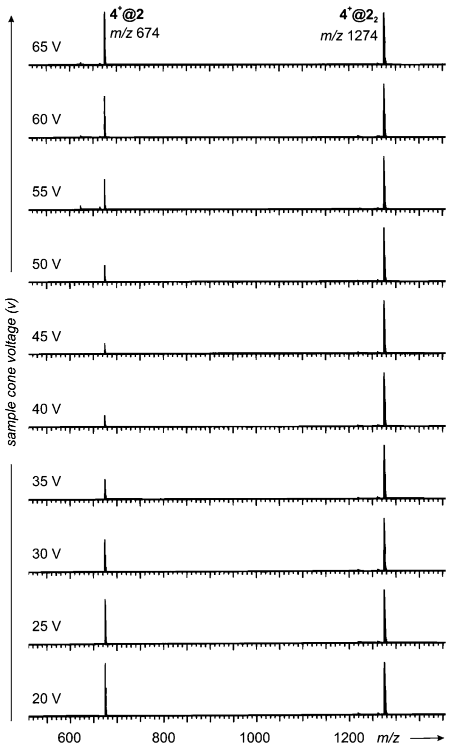

Fig. 9 In-source fragmentation behaviour of 4^+@**2** and 4^+@$\mathbf{2}_2$ and its dependence on the sample cone voltage. The sample cone voltage rises from 20 (bottom) to 65 V (top) in steps of 5 V. Reproducibly, the signal for the monomer–guest complex 4^+@**2** first decreases in intensity relative to the corresponding dimer–guest complex, but at higher sample cone voltages increases again.

to similar results. In order to even further support the assumption of the formation of capsular ions that are stable even under environment-free conditions, *i.e.* in the absence of solvent molecules and counterions, the fragmentation behaviour has been investigated. Since our instrument does not allow for MS/MS experiments, we applied different voltages to the sample cone of the instrument in order to induce in-source fragmentation. Before entering the first vacuum pumping stage through the sample cone, the ions move through an ion source housing kept at about ambient pressure. If the voltage applied to the sample cone is low, the ions are not significantly accelerated and undergo fragmentations only to a minor extent upon collisions with the surrounding gas molecules. With a high sample cone voltage, however, the ions approach the sample cone at a higher velocity and collisions with the surrounding gas lead to much more pronounced fragmentations.

Fig. 9 summarizes the results from these experiments. Starting at a sample cone voltage of 20 V, in the spectrum obtained from a solution of 4^+Br^- and **1**, the monomer–guest complex 4^+@**2** and the capsule 4^+@$\mathbf{2}_2$ appear with almost the same abundance. Upon stepwise increase of the voltage to 45 V with increments of 5 V, the monomer–guest complex decreases significantly in intensity relative to its dimeric counterpart. Finally, an estimated 1:5 ratio is obtained. Further increase of the sample cone voltage, however, did not lead to a further decrease in 4^+@**2** intensity. Rather, the intensity of this ion increases and at 65 V reaches again the 1:1 ratio of the beginning. These results can be rationalized by assuming that the monomer–guest complex fragments into the "naked" cation and a neutral resorcinarene at lower energy as compared to the dimer–guest complex. That would explain the marked decrease in its intensity. At lower collision energies, first the monomer complex would be destroyed. Upon increase of the collision energy, at a certain point enough energy is provided for the decomposition of the dimer–guest complex into a neutral resorcinarene and the corresponding monomer–guest complex. This would regenerate the latter and thus also explain why its intensity increases at even higher voltages. If this scenario holds true, it means that the cation is bound more tightly to the resorcinarene dimer than to the monomer. This is only in line with a structure where the cation is inside a cavity and protected against release by additional forces, which presumably come from the seam of hydrogen bonding between the two resorcinarenes. A very similar behaviour has been observed for hydrogen-bonded calixarene capsules before and led to the same conclusions.[11b] Note, however, that the observed fragmentation of the dimer–guest complex to yield the monomer–guest complex is probably not the fragmentation process of lowest energy. More likely, the release of the guest cation, *i.e.* the loss of the complete capsule, has a lower barrier but the collisions in the ion source region may well open reaction channels higher than the lowest-energy fragmentation pathways.

Control experiment and negative ion ESI spectra. There is an excellent control experiment confirming that the cation does not bind easily to the outer surface. A resorcinarene O–CH_2–O-bridged at the upper rim by four acetal methylene groups bears a fixed conformation very close to that of the merely hydrogen-bonded analogue. Consequently, one might expect to see binding to this host in the form of its monomer–guest complex, while the resorcinarenes cannot dimerise any more since they lack the capability of hydrogen bond formation. However, no signal at all is observed for the monomer–guest or dimer–guest complex. This behaviour can easily be explained by the methylene bridges pointing inwards and thus blocking the cavity against access of the cation. Consequently, the only binding mode in this case would be binding of the cation to the outer surface of the resorcinarene. The absence of any signal for the monomer–guest complex reveals that this is indeed not feasible.

Finally, it should be noted that capsules are not only formed as positive ions. The negative ion spectrum obtained with **1** and tetramethyl ammonium as the guest salt provides an interesting additional aspect (Fig. 10). Ions are observed that correspond to doubly deprotonated resorcinarenes binding tightly an ammonium ion in a 4^+[@**1**$-2H^+$] complex at m/z 616. Accordingly, the dimer 4^+[@**1**$-H^+$]$_2$ (m/z 1160) is also formed with quite considerable abundance. The net charge of these complexes is -1. Weaker in intensity, but still clearly visible is a signal for a singly-deprotonated dimer 4^+Br^-@[$\mathbf{1}_2$$-H^+$] ($m/z$ 1242) which receives its negative charge from an attached bromide ion. A further member in this series is $4^+Br^-_2$@$\mathbf{1}_2$ at

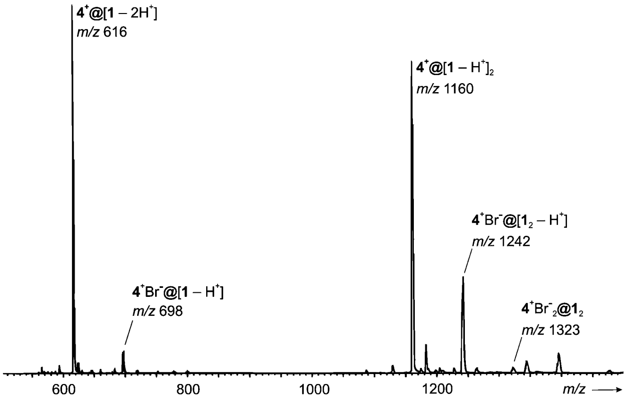

Fig. 10 Negative ion ESI mass spectrum of a 50 μM solution of **1** containing tetramethyl ammonium bromide as the guest salt (50 μM).

m/z 1323. In this complex both resorcinarenes are neutral. The positive charge of the ammonium ion is overcompensated by complexation of two bromide ions. Although we do not have any structural information from the mass spectrometric experiments, these complexes are of particular interest, because partial deprotonation of the resorcinarenes may well increase the strength of the hydrogen bonds connecting them and thus stabilize a capsule significantly as compared to its neutral relatives.

Conclusions

In conclusion, a total of eight crystal structures of dimeric molecular capsules formed by resorcinarenes **1**, **2** and **3** with small ammonium cations $\mathbf{4}^+$ and $\mathbf{5}^+$ in aqueous methanol and ethanol solutions were determined. All capsules are mediated by hydrogen-bonded networks *via* solvent and in most cases also *via* spherical counter anions. C–H···π and cation-π interactions probably act as a capsule forming driving force since several weak interactions between the aromatic parts of the host and the carbons of the guest are evident on the basis of their closest distances.

The only host capable of binding the spherical anion at the lower rim alkyl chain is **2**, which indicates that the methyl group of **1** is too short and bulky for anion binding while propyl chains of **3** already start to pack as intervening hydrophobic layers typical to longer alkyl chain resorcinarenes such as C11.[18]

Half of the capsules possess staggered structures, which supposedly should be tighter, *i.e.* capsule halves should be drawn closer together. However, staggered capsule $\mathbf{4@2_2}\cdot\mathrm{Cl^-}\cdot 6\mathrm{MeOH}\cdot\mathrm{H_2O}$ is significantly looser than other staggered capsules and, as well, eclipsed capsule $\mathbf{4@3_2}\cdot\mathrm{Cl^-}\cdot 4\mathrm{EtOH}$ is significantly tighter than other eclipsed capsules (Table 2). Thus, no direct conclusion about the spatial orientation of the capsule halves and the tightness of the capsule can be drawn. It seems that the interplay of cations, anions and solvents used gives rather unpredictable results with no straightforward pattern – except for the relatively easy capsule formation in all cases. Still, it is reasonable to assume that by using bigger cations, such as the tetraethyl ammonium cation (**6**) and 1,4-dimethyl-1,4-diazoniabicyclo[2.2.2]octane,[3d] and bulkier solvents, such as ethanol, the formation of an eclipsed oriented capsule is favoured.

With mass spectrometric experiments, we provide several different pieces of evidence which speak in favour of capsule formation not only in the solid state, but also in solution and even in the gas phase: size selectivity, heterodimer formation, and fragmentation behaviour. Of course, structural evidence coming from mass spectrometric experiments is necessarily indirect and somewhat limited, but on the other hand, these experiments also demonstrate the power of this technique beyond mere determination of accurate molecular masses. One might speculate what the binding forces are which hold the capsular structure together and make it stable enough to be intactly transferred into the gas phase. Likely, the seam of hydrogen bonds is not the only force "at work". Cation-π and C–H···π interactions are known to stabilize such assemblies significantly.[6,11,12]

Our future tasks include using even smaller cations than TMA and searching for different crystallisation conditions to obtain perhaps even tighter capsules. NMR competitive and titration experiments are underway to complement these studies in solution.

Experimental

Crystal structures

Suitable single crystals for X-ray analysis were obtained by slow evaporation of the aqueous methanol or ethanol solutions (Table 1).

The X-ray crystallographic data for all complexes were recorded with a Nonius Kappa CCD diffractometer. Graphite monochromatised MoK$_\alpha$ radiation [$\lambda(\mathrm{MoK_\alpha}) = 0.71073$ Å] and temperature of 173.0 ± 0.1 K were used in all cases. The CCD data were processed with Denzo-SMN v0.95.373[18a] and all structures were solved by direct methods (SHELXS-97[18b])

Table 3 Crystal data and collection parameters

Capsule	$\mathbf{4}^+@\mathbf{1}_2\cdot\mathrm{Br^-}\cdot 4\mathrm{MeOH}\cdot 3\mathrm{H_2O}$	$\mathbf{4}^+@\mathbf{2}_2\cdot\mathrm{Cl^-}\cdot 6\mathrm{MeOH}\cdot\mathrm{H_2O}$	$\mathbf{4}^+@\mathbf{2}_2\cdot\mathrm{Cl^-}\cdot 4.5\mathrm{H_2O}$	$\mathbf{4}^+@\mathbf{2}_2\cdot\mathrm{Br^-}\cdot 8\mathrm{MeOH}$	$\mathbf{4}^+@\mathbf{3}_2\cdot\mathrm{Cl^-}\cdot 4\mathrm{MeOH}$	$\mathbf{4}^+@\mathbf{3}_2\cdot\mathrm{Cl^-}\cdot 4\mathrm{EtOH}$	$\mathbf{4}^+@\mathbf{3}_2\cdot\mathrm{Br^-}\cdot 4\mathrm{EtOH}$	$\mathbf{5}^+@\mathbf{3}_2\cdot\mathrm{Br^-}\cdot 4\mathrm{MeOH}\cdot 0.5\mathrm{H_2O}$
Formula	$2\mathrm{C_{32}H_{32}O_8}\cdot\mathrm{C_4H_{12}N^+Br^-}\cdot 4\mathrm{CH_3OH}\cdot 3\mathrm{H_2O}$	$2\mathrm{C_{36}H_{40}O_8}\cdot\mathrm{C_4H_{12}N^+Cl^-}\cdot 6\mathrm{CH_3OH}\cdot\mathrm{H_2O}$	$2\mathrm{C_{36}H_{40}O_8}\cdot\mathrm{C_4H_{12}N^+Cl^-}\cdot 4.5\mathrm{H_2O}$	$2\mathrm{C_{36}H_{40}O_8}\cdot\mathrm{C_4H_{12}N^+Br^-}\cdot 8\mathrm{CH_3OH}$	$2\mathrm{C_{40}H_{48}O_8}\cdot\mathrm{C_4H_{12}N^+Cl^-}\cdot 4\mathrm{CH_3OH}$	$2\mathrm{C_{40}H_{48}O_8}\cdot\mathrm{C_4H_{12}N^+Cl^-}\cdot 4\mathrm{C_2H_5OH}$	$2\mathrm{C_{40}H_{48}O_8}\cdot\mathrm{C_4H_{12}N^+Br^-}\cdot 4\mathrm{C_2H_5OH}$	$2\mathrm{C_{40}H_{48}O_8}\cdot\mathrm{C_6H_{18}N^+Br^-}\cdot 4\ \mathrm{C_2H_5OH}\cdot 0.5\mathrm{H_2O}$
M	1407.4	1521.3	1392.0	1611.8	1551.3	1607.4	1651.9	1634.9
a/Å	14.2645(7)	27.4410(4)	13.6265(3)	14.2230(7)	22.4960(4)	13.3702(4)	13.3833(2)	13.2301(2)
b/Å	14.2675	27.4283(6)	14.2716(2)	14.2230	13.7567(3)	13.7036(4)	13.7536(2)	13.5456(3)
c/Å	18.4532(9)	26.0750(5)	20.8343(4)	21.547(2)	27.7823(6)	14.4145(7)	14.4512(3)	14.7790(4)
α/°	90	90	90	90	90	106.713(2)	106.6801(5)	105.8011(6)
β/°	90	121.702(2)	90	90	100.656(1)	90.504(2)	91.0839(5)	90.7846(7)
γ/°	90	90	90	90	90	117.936(2)	117.2219(5)	118.409(1)
V/Å^3	3754.8(3)	16 697.3(5)	4051.7(1)	4358.9(4)	8449.5(3)	2202.3(1)	2230.4(1)	2209.2(1)
Z	2	8	2	2	4	1	1	1
Crystal system	Tetragonal	Monoclinic	Orthorhombic	Tetragonal	Monoclinic	Triclinic	Triclinic	Triclinic
Space group	$P\bar{4}\ _2/c$	$C2/c$	$Pnnn$	$I4/m$	$C2/c$	$P\bar{1}$	$P\bar{1}$	$P\bar{1}$
D_c/Mg m^{-3}	1.245	1.196	1.141	1.228	1.219	1.212	1.230	1.229
μ/mm^{-1}	0.619	0.116	0.114	0.543	0.115	0.113	0.530	0.534
Reflections measured/unique	13 197/3284	19 652/13 270	11 402/3237	9057/1978	17 904/7253	12 026/7692	12 083/7741	12 471/7769
Refl. used in refinement[a]	2233	5670	2223	1333	3703	4028	5376	5162
R_{int}	0.073	0.069	0.063	0.063	0.108	0.047	0.039	0.044
R/R_{w}[b]	0.088/0.223	0.092/0.207	0.108/0.295	0.094/0.267	0.073/0.191	0.079/0.200	0.065/0.168	0.072/0.175
No. of parameters	217	1007	232	136	503	548	531	525
GooF	1.068	1.040	1.062	1.101	0.998	1.021	1.027	1.040

[a] $I > 2\sigma(I)$. [b] For data $I > 2\sigma(I)$.

and refined on F^2 by full-matrix least-squares techniques (SHELXL-97[18c]). The hydrogen atoms were calculated to their idealised positions with isotropic temperature factors (1.2 or 1.5 times the carbon temperature factor) and refined as riding atoms. Hydrogen atoms for any water molecules were not determined.

Carbon atoms of the cations of $\mathbf{4}^{+}@\mathbf{2}_{2}\cdot Cl^{-}\cdot 4.5H_{2}O$, $\mathbf{4}^{+}@\mathbf{2}_{2}\cdot Br^{-}\cdot 8MeOH$, $\mathbf{4}^{+}@\mathbf{3}_{2}\cdot Cl^{-}\cdot 4EtOH$, $\mathbf{4}^{+}@\mathbf{3}_{2}\cdot Br^{-}\cdot 4EtOH$, $\mathbf{5}^{+}@\mathbf{3}_{2}\cdot Br^{-}\cdot 4MeOH\cdot 0.5H_{2}O$ and $\mathbf{4}^{+}@\mathbf{2}_{2}\cdot Cl^{-}\cdot 6MeOH\cdot H_{2}O$ and disordered solvent molecules for structures $\mathbf{4}^{+}@\mathbf{3}_{2}\cdot Br^{-}\cdot 4EtOH$, $\mathbf{4}^{+}@\mathbf{2}_{2}\cdot Cl^{-}\cdot 4.5H_{2}O$, $\mathbf{4}^{+}@\mathbf{2}_{2}\cdot Cl^{-}\cdot 6MeOH\cdot H_{2}O$ and $\mathbf{4}^{+}@\mathbf{3}_{2}\cdot Cl^{-}\cdot 4EtOH$ were treated isotropically. The cations of $\mathbf{4}^{+}@\mathbf{2}_{2}\cdot Cl^{-}\cdot 4.5H_{2}O$, $\mathbf{4}^{+}@\mathbf{2}_{2}\cdot Br^{-}\cdot 8MeOH$, $\mathbf{4}^{+}@\mathbf{3}_{2}\cdot Cl^{-}\cdot 4EtOH$, $\mathbf{4}^{+}@\mathbf{3}_{2}\cdot Br^{-}\cdot 4EtOH$ and $\mathbf{5}^{+}@\mathbf{3}_{2}\cdot Br^{-}\cdot 4MeOH\cdot 0.5H_{2}O$ are disordered and no hydrogen atoms were determined for these cations. Bromide–chloride and one of the water molecules are disordered between themselves in $\mathbf{4}^{+}@\mathbf{1}_{2}\cdot Br^{-}\cdot 4MeOH\cdot 3H_{2}O$ and in $\mathbf{4}^{+}@\mathbf{2}_{2}\cdot Cl^{-}\cdot 6MeOH\cdot H_{2}O$. However, in the later one the disorder is treated solely as chloride to keep the refinement stabile.

Residual electron density below 1.30 e Å^{-3} was found in $\mathbf{4}^{+}@\mathbf{2}_{2}\cdot Br^{-}\cdot 8MeOH$ close to the Br^{-} atom, in $\mathbf{4}^{+}@\mathbf{2}_{2}\cdot Cl^{-}\cdot 4.5H_{2}O$ close to the cation and in $\mathbf{5}^{+}@\mathbf{2}_{2}\cdot Cl^{-}\cdot 4MeOH\cdot 0.5H_{2}O$ O close to disordered methanol carbon.

In structures $\mathbf{4}^{+}@\mathbf{2}_{2}\cdot Br^{-}\cdot 8MeOH$ and $\mathbf{5}^{+}@\mathbf{3}_{2}\cdot Br^{-}\cdot 4MeOH\cdot 0.5H_{2}O$ one geometrical restraint was used to keep the disordered cation chemically reasonable. See Table 3 for detailed crystallographic data.

CCDC reference numbers 196091–196098.

See http://www.rsc.org/suppdata/nj/b2/b207875a/ for crystallographic data in CIF or other electronic format.

LCT ESI-TOF mass spectra

The mass spectrometric experiments were performed with a Micromass LCT ESI-TOF instrument equipped with a Z geometry electrospray ion source. For both positive and negative ion spectra, the samples were introduced into the source as acetonitrile solutions of the monomers **1**–**3** (50 μM) and the salts $\mathbf{4}^{+}Br^{-}$ – $\mathbf{7}^{+}Br^{-}$ (50 μM) at flow rates of 15 μL min^{-1}. A constant spray and highest intensities were achieved with a capillary voltage of 3700 V at a source temperature of 80 °C and a desolvation temperature of 120 °C. Other selected source parameters were as follows: sample cone voltage: 20–30 V, extraction cone voltage: 3–6 V, flow of cone gas: 10 L h^{-1}, flow of desolvation gas: 150 L h^{-1}. Other parameters did not influence the ion intensities much. The sample cone voltage was optimized at a somewhat higher value of 50 V for negative ion spectra. For the examination of heterodimer formation, two of the sample solutions were mixed in a 1:1 ratio and then subjected to the same experiments. Competition experiments with two different guests were performed with solutions containing the capsule monomers (50 μM) and each guest at 100 μM concentrations, *i.e.* in fourfold excess relative to the dimeric capsules. Since only qualitative data were required, no corrections with respect to ESI response factors were done.[19] It is assumed that these are similar for the capsules under study when only the guest cation is exchanged. In particular, this can be expected to be true for capsules, where the guest ion is located inside a host, which is the same for all ions in such a competition experiment. Multiple scans (50–200) were recorded and averaged for each spectrum in order to improve the signal-to-noise ratio.

Since the instrument does not permit MS/MS experiments, the fragmentation behaviour of the samples was examined by in-source fragmentation induced by collisions with the gas molecules present in the ion source. For this purpose, the ions were accelerated to different kinetic energies through tuning the sample cone voltage accordingly. At high voltages, the ions undergo collisions at higher velocities and usually pronounced fragmentation is observed.

Acknowledgements

We thank M.Sc. M. Luostarinen, Dr. D. Falàbu and Ph.Lic. J. Ropponen for providing compounds **1**, **2**, and **5**, respectively. The financial support of The Graduate School of Bioorganic Chemistry (H. M.) and Academy of Finland (project no. 100319; M. N.) are gratefully acknowledged. C.A.S. is grateful for fellowship support by the Fonds der Chemischen Industrie (Liebig fellowship) and the German Academic Exchange Service (DAAD). Part of the work has been funded by the Deutsche Forschungsgemeinschaft.

References

1 (*a*) M. Morgan Conn and J. Rebek, Jr., *Chem. Rev.*, 1997, **97**, 1647; (*b*) F. Hof, S. L. Craig, C. Nuckolls and J. Rebek, Jr., *Angew. Chem., Int. Ed.*, 2002, **41**, 1488.

2 P. Timmerman, W. Verboom and D. N. Reinhouldt, *Tetrahedron*, 1996, **52**, 2663.

3 (*a*) K. Murayama and K. Aoki, *Chem. Commun.*, 1998, 607; (*b*) A. Shivanyuk, K. Rissanen and E. Kolehmainen, *Chem. Commun.*, 2000, 1107; (*c*) A. Shivanyuk and J. Rebek, Jr., *Chem. Commun.*, 2001, 2374; (*d*) H. Mansikkamäki, M. Nissinen and K. Rissanen, *Chem. Commun.*, 2002, 1902–1903.

4 (*a*) L. R. MacGillvray and J. L. Atwood, *Nature*, 1997, **389**, 469; (*b*) A. Shivanyuk and J. Rebek, Jr., *Chem. Commun.*, 2001, 2424; (*c*) A. Shivanyuk and J. Rebek, Jr., *Proc. Natl. Acad. Sci. USA*, 2001, **98**, 2374; (*d*) T. Gerkensmeier, W. Iwanek, C. Agena, R. Fröhlich, S. Kotila, C. Näther and J. Mattay, *Eur. J. Org. Chem.*, 1999, 2257.

5 (*a*) K. Murayama and K. Aoki, *Chem. Commun.*, 1997, 119; (*b*) H.-J. Schneider, D. Güttes and U. Schneider, *Angew. Chem., Int. Ed. Engl.*, 1986, **25**, 647; (*c*) H.-J. Schneider, D. Güttes and U. Schneider, *J. Am. Chem. Soc.*, 1988, **110**, 6449; (*d*) U. Schneider and H.-J. Schneider, *Chem. Ber.*, 1994, **127**, 2455.

6 M. Mäkinen, M. Nissinen, K. Rissanen and P. Vainiotalo, *J. Am. Soc. Mass Spectrom.*, submitted.

7 For reviews on the application of mass spectrometry to different aspects in host–guest and supramolecular chemistry, see (*a*) J. S. Brodbelt and C.-C. Liou, *Pure Appl. Chem.*, 1993, **65**, 409; (*b*) D. V. Dearden, H. Zhang, I.-H. Chu, P. Wong and Q. Chen, *Pure Appl. Chem.*, 1993, **65**, 423; (*c*) J. S. Brodbelt and D. V. Dearden, *Mass Spectrometry in: Comprehensive Supramolecular Chemistry*, ed. J. L. Atwood, J. E. D. Davies, D. D. MacNicol, F. Vögtle, J.-M. Lehn, and J. A. Ripmeester, Pergamon, Oxford, 1996, vol. 8, 567; (*d*) M. Przybylski and M. O. Glocker, *Angew. Chem.*, 1996, **108**, 878; *Angew. Chem., Int. Ed. Eng.*, 1996, 35, 806; (*e*) J. S. Brodbelt, *Int. J. Mass Spectrom.*, 2000, **200**, 57; (*f*) C. A. Schalley, *Int. J. Mass Spectrom.*, 2000, **194**, 11–39; (*j*) C. B. Lebrilla, *Acc. Chem. Res.*, 2001, **34**, 653; (*g*) C. A. Schalley, *Mass Spectrom. Rev.*, 2001, **20**, 253.

8 (*a*) K. C. Russell, E. Leize, A. Van Dorsselaer and J.-M. Lehn, *Angew. Chem.*, 1995, **107**, 244; K. C. Russell, E. Leize, A. Van Dorsselaer and J.-M. Lehn, *Angew. Chem., Int. Ed. Eng.*, 1995, **34**, 209; (*b*) X. Cheng, Q. Gao, R. D. Smith, E. E. Simanek, M. Mammen and G. M. Whitesides, *Rapid Commun. Mass. Spectrom.*, 1995, **9**, 312; (*c*) X. Cheng, Q. Gao, R. D. Smith, E. E. Simanek, M. Mammen and G. M. Whitesides, *J. Org. Chem.*, 1996, **61**, 2204.

9 (*a*) P. Timmerman, R. H. Vreekamp, R. Hulst, W. Verboom, D. N. Reinhoudt, K. Rissanen, K. A. Udachin and J. Ripmeester, *Chem. Eur. J.*, 1997, **3**, 1823; (*b*) K. A. Joliffe, M. Crego Calama, R. Fokkens, N. M. M. Nibbering, P. Timmerman and D. N. Reinhoudt, *Angew. Chem.*, 1998, **110**, 1294; K. A. Joliffe, M. Crego Calama, R. Fokkens, N. M. M. Nibbering, P. Timmerman and D. N. Reinhoudt, *Angew. Chem., Int. Ed.*, 1998, **37**, 1247; (*c*) P. Timmerman, K. A. Joliffe, M. Crego Calama, J.-L. Weidmann, L. J. Prins, F. Cardullo, B. H. M. Snellink-Ruël, R. H. Fokkens, N. M. M. Nibbering and S. Shinkai, *Chem. Eur. J.*, 2000, **6**, 4104.

10 M. Scherer, J. L. Sessler, M. Moini, A. Gebauer and V. Lynch, *Chem. Eur. J.*, 1998, **4**, 152.

11 (*a*) C. A. Schalley, J. M. Rivera, T. Martín, J. Santamaría, G. Siuzdak and J. Rebek, Jr., *Eur. J. Org. Chem.*, 1999, 1325; (*b*) C. A. Schalley, R. K. Castellano, M. S. Brody, D. M. Rudkevich,

G. Siuzdak, J. Rebek, Jr., *J. Am. Chem. Soc.*, 1999, **121**, 4568; (*c*) M. S. Brody, D. M. Rudkevich, C. A. Schalley and J. Rebek, Jr., *Angew. Chem.*, 1999, **111**, 1738; M. S. Brody, D. M. Rudkevich, C. A. Schalley and J. Rebek, Jr., *Angew. Chem., Int. Ed.*, 1999, **38**, 1640; (*d*) C. A. Schalley, T. Martín, U. Obst and J. Rebek, Jr., *J. Am. Chem. Soc.*, 1999, **121**, 2133; (*e*) A. Lützen, A. R. Renslo, C. A. Schalley, B. M. O'Leary and J. Rebek, Jr., *J. Am. Chem. Soc.*, 1999, **121**, 7455; (*f*) B. M. O'Leary, T. Szabo, N. Svenstrup, C. A. Schalley, A. Lützen and J. Rebek, Jr., *J. Am. Chem. Soc.*, 2001, **123**, 11 519.

12 (*a*) J. A. Bryant, M. T. Blanda, M. Vincenti and D. J. Cram, *J. Am. Chem. Soc.*, 1991, **113**, 2167; (*b*) L. M. Nuwaysir, J. A. Castoro, C. L.-C. Yang and C. L. Wilkins, *J. Am. Chem. Soc.*, 1992, **114**, 5748; (*c*) F. Inokuchi, Y. Shiomi, H. Kawabata, T. Sakaki and S. Shinkai, *Chem. Lett.*, 1993, 1595; (*d*) F. Inokuchi, K. Araki and S. Shinkai, *Chem. Lett.*, 1994, 1383; (*e*) F. Inokuchi, Y. Miyahara, T. Inazu and S. Shinkai, *Angew. Chem.*, 1995, **107**, 1459; F. Inokuchi, Y. Miyahara, T. Inazu and S. Shinkai, *Angew. Chem., Int. Ed. Engl.*, 1994, **34**, 1364; (*f*) P. S. H. Wong, X. Yu and D. V. Dearden, *Inorg. Chim. Acta*, 1996, **246**, 259; (*g*) R. Warmuth, *Chem. Commun.*, 1998, 59; (*h*) A. Irico, M. Vincenti and E. Dalcanale, *Chem. Eur. J.*, 2001, **7**, 2034; (*i*) M. C. Letzel, C. Agena and J. Mattay, *Eur. J. Mass Spectrom.*, 2001, **7**, 35; (*j*) E. Ventola, K. Rissanen and P. Vainiotalo, *Chem. Commun.*, 2002, 1110; (*k*) M. Mäkinen, P. Vainiotalo and K. Rissanen, *J. Am. Soc. Mass Spectrom.*, 2002, **7**, 851.

13 (*a*) M. Vincenti, E. Dalcanale, P. Soncini and G. Guglielmetti, *J. Am. Chem. Soc.*, 1990, **112**, 445; (*b*) M. Vincenti, E. Pelizzetti, E. Dalcanale and P. Soncini, *Pure Appl. Chem.*, 1993, **65**, 1507; (*c*) M. Vincenti, *J. Mass Spectrom.*, 1995, **30**, 925; (*d*) M. Vincenti, C. Minero, E. Pelizzetti, A. Secchi and E. Dalcanale, *Pure Appl. Chem.*, 1995, **67**, 1075; (*e*) M. Vincenti and E. Dalcanale, *J. Chem. Soc., Perkin Trans. 2*, 1995, 1069; (*f*) A. Arduini, M. Cantoni, E. Graviani, A. Pochini, A. Secchi, A. R. Sicuri, R. Ungaro and M. Vincenti, *Tetrahedron*, 1995, **51**, 599; (*g*) M. Vincenti, A. Irico and E. Dalcanale, *Adv. Mass Spectrom.*, 1998, **14**, 129; (*h*) J. M. J. Nuutinen, A. Irico, M. Vincenti, E. Dalcanale, J. H. M. Pakarinen and P. Vainiotalo, *J. Am. Chem. Soc.*, 2000, **122**, 10 090; (*i*) A. Irico and M. Vincenti, *Int. J. Mass Spectrom.*, 2002, **214**, 23.

14 M. C. Letzel, C. Agena and J. Mattay, *J. Mass Spectrom.*, 2002, **37**, 63.

15 H. Mansikkamäki, M. Nissinen and K. Rissanen, unpublished results.

16 ORTEP3 for Windows – L. J. Farrugia, *J. Appl. Crystallogr.*, 1997, **30**, 565.

17 H. Adams, F. Davis and C. J. M. Stirling, *Chem. Commun.*, 1994, 2527.

18 (*a*) Z. Otwinowski and W. Minor in *Processing of X-ray Diffraction Data Collected in Oscillation Mode, Methoods in Enzymology, vol. 276: Macromolecular Chrystallography*, Part A, ed. C. W. Carter, Jr. and R. M. Sweet, Academic Press, New York, 1997, 307; (*b*) G. M. Sheldrick, SHELXS-97, A program for Automatic Solution of Crystal Structures, University of Göttingen, Germany, 1997; (*c*) G. M. Sheldrick, SHELXS-97, A program for Crystal Structure Refinement, University of Göttingen, Germany, 1997.

19 E. Leize, A. Jaffrezic and A. Van Dorsselaer, *J. Mass Spectrom.*, 1996, **31**, 53.